physica status solidi c

www.pss-c.com

current topics in solid state physics

Near-field second-harmonic generation from gold nanoellipsoids

M. Celebrano[1], P. Biagioni[2], M. Finazzi[2], L. Duò[2], M. Zavelani-Rossi[1], D. Polli[1], M. Labardi[3], M. Allegrini[3], J. Grand[4], P.-M. Adam[4], P. Royer[4], and G. Cerullo[1]

[1] Istituto di Fotonica e Nanotecnologie, CNR, Dipartimento di Fisica, Politecnico di Milano, Piazza Leonardo Da Vinci 32, 20133 Milano, Italy
[2] LNESS – Dipartimento di Fisica, Politecnico di Milano, Piazza Leonardo Da Vinci 32, 20133 Milano, Italy
[3] CNR-INFM, polyLab, Dipartimento di Fisica "Enrico Fermi", Università di Pisa, Largo Pontecorvo 3, 56127 Pisa, Italy
[4] Laboratoire de Nanotechnologie et d'Instrumentation Optique, Université de Technologie de Troyes, 12 rue Marie Curie, BP 2060 10010 Troyes cedex, France

Received 3 August 2007, revised 14 November 2007, accepted 3 December 2007
Published online 21 May 2008

PACS 42.65.Ky, 42.65.Re, 61.46.Df, 68.37.Uv

Second-harmonic generation from single gold nanofabricated particles is experimentally investigated by a nonlinear scanning near-field optical microscope (SNOM). High peak power femtosecond polarized light pulses at the output of a hollow pyramid aperture allow for efficient second-harmonic imaging, with sub-100-nm spatial resolution and high contrast. The near-field nonlinear response is found to be directly related to both local surface plasmon resonances and particle morphology. The combined analysis of linear and second-harmonic SNOM images allows one to discriminate among near-field scattering, absorption and re-emission processes, which would not be possible with linear techniques alone.

phys. stat. sol. (c) **5**, No. 8, 2657–2661 (2008) / **DOI** 10.1002/pssc.200779121

WILEY-VCH

phys. stat. sol. (c) **5**, No. 8, 2657–2661 (2008) / **DOI** 10.1002/pssc.200779121

physica status solidi c
www.pss-c.com
current topics in solid state physics

Near-field second-harmonic generation from gold nanoellipsoids

M. Celebrano[1], P. Biagioni[*,2], M. Finazzi[2], L. Duò[2], M. Zavelani-Rossi[1], D. Polli[1], M. Labardi[3], M. Allegrini[3], J. Grand[4], P.-M. Adam[4], P. Royer[4], and G. Cerullo[1]

[1] Istituto di Fotonica e Nanotecnologie, CNR, Dipartimento di Fisica, Politecnico di Milano, Piazza Leonardo Da Vinci 32, 20133 Milano, Italy
[2] LNESS – Dipartimento di Fisica, Politecnico di Milano, Piazza Leonardo Da Vinci 32, 20133 Milano, Italy
[3] CNR-INFM, polyLab, Dipartimento di Fisica "Enrico Fermi", Università di Pisa, Largo Pontecorvo 3, 56127 Pisa, Italy
[4] Laboratoire de Nanotechnologie et d'Instrumentation Optique, Université de Technologie de Troyes, 12 rue Marie Curie, BP 2060 10010 Troyes cedex, France

Received 3 August 2007, revised 14 November 2007, accepted 3 December 2007
Published online 21 May 2008

PACS 42.65.Ky, 42.65.Re, 61.46.Df, 68.37.Uv

* Corresponding author: e-mail paolo.biagioni@polimi.it

Second-harmonic generation from single gold nanofabricated particles is experimentally investigated by a nonlinear scanning near-field optical microscope (SNOM). High peak power femtosecond polarized light pulses at the output of a hollow pyramid aperture allow for efficient second-harmonic imaging, with sub-100-nm spatial resolution and high contrast. The near-field nonlinear response is found to be directly related to both local surface plasmon resonances and particle morphology. The combined analysis of linear and second-harmonic SNOM images allows one to discriminate among near-field scattering, absorption and re-emission processes, which would not be possible with linear techniques alone.

1 Introduction The rapid development of nanoscience and nanotechnology during the last years has stimulated research on the analysis of electromagnetic fields that show up at the nanoscale, and the development of tools for studying and exploiting them in order to obtain new compact and all-optical devices [1, 2]. The interaction of light with metal nanostructures is known to produce strong (up to several orders of magnitude) and spatially localized (on nanometer scale) field intensity enhancement. These enhancements can be due to local coupling of light with particular resonant structures (antenna effect) [3] or to field concentration on structures with strong curvature (lightning-rod effect) [4]. A further effect is the resonant excitation of the so-called Localized Surface Plasmons (LSPs) [5]; the resonance frequencies of the LSP can be tailored in a broad spectral range according to the material and shape of the nanostructure. Local field enhancements (LFEs) are best observed exploiting nonlinear optical effects, such as Second-Harmonic Generation (SHG) [6-10] or Two-Photon Photo-Luminescence (TPPL) [7, 11, 12] which depend on the square of the light intensity. In order to observe a significant non-linear response, the samples need to be illuminated by high peak intensities such as those associated with very short laser pulses.

The nonlinear optical response of nanostructured surfaces has been studied both theoretically [13-15] and experimentally by confocal optical microscopy [16-18]. Far-field techniques, however, are limited by diffraction, which prevents the study of high density patterned samples and do not allow for direct mapping of optical field distributions in the near-field, where they show the highest intensity. A Scanning Near-field Optical Microscope (SNOM) is a more suitable tool to such purpose, allowing one to probe optical fields in the proximity of scatterers' interfaces; moreover, it is able to overcome the diffraction limit by confining the light on the nanometer scale [19, 20] and to provide simultaneous information on the sample topography.

In this paper we use a novel setup for nonlinear near-field microscopy to map LFEs on metal nanostructures. In this apparatus, femtosecond pulses are coupled to a SNOM head employing hollow-pyramid aperture probes that ex-

hibit the unique feature of preserving pulse duration [21] and light polarization [22]. This enables the achievement of high peak power in the near field, a prerequisite for the efficient generation of nonlinear optical effects. We use such a system to observe the nonlinear optical response of nanofabricated gold ellipsoids with sub-100-nm spatial resolution; in fact, nonlinear effects and in particular SHG are well known to be very efficient probes for LFE detection.

The nanoellipsoids have different lengths in order to tune their LSP resonance frequency with respect to the fixed excitation wavelength of the laser pulses. Particular attention is paid to discriminate between LSP-induced LFE and other mechanisms (e.g. lightning rod effects) which can as well provide large field intensities in the proximity of the nanoparticle.

2 Experimental

2.1 Experimental setup A sketch of the experimental setup is shown in Fig. 1. The excitation light is generated by a standard asymmetric Ti:sapphire oscillator in a stretched cavity configuration used to decrease the repetition rate down to 26 MHz. For a given average power, as limited by thermal effects in the near-field probe, this allows increasing the peak power by a factor of ~4 with respect to a standard 100-MHz cavity, enhancing second-order nonlinear optical effects by the same factor. The oscillator produces ~30 fs pulses with energy up to 20 nJ. These are sent to a pre-compressor, consisting of a double pass in a Brewster-cut fused-silica prism pair, to compensate for the dispersion introduced by the optical elements in the path to the sample, as shown in Fig. 1.

The beam is then coupled to our home-made SNOM based on cantilevered probes, consisting of hollow pyramids made of silicon oxide coated with aluminium with an aperture at the apex ranging between 60 and 200 nm [23], and throughputs up to 5×10^{-3}. Tip/sample distance stabilization is performed by measuring cantilever deflection with the optical lever method, like in atomic force microscopy (AFM).

After the optical interaction with the sample, the transmitted fundamental wavelength (FW) as well as the induced SHG are collected by a 0.8-NA microscope objective, separated by proper filtering, and simultaneously measured by two photo-multiplier tubes. The FW passes through a pinhole to reject stray light in a confocal-like detection configuration; SHG is reflected by a dichroic mirror (reflectivity > 95% at $\lambda < 410$ nm) and then selected through an interference filter at 400 nm ($\Delta\lambda = 30$ nm). The average incident power on the tip during scans was ~1 mW, below the probe damaging threshold. This allowed us to efficiently induce nonlinear effects in the near field of the probe [24].

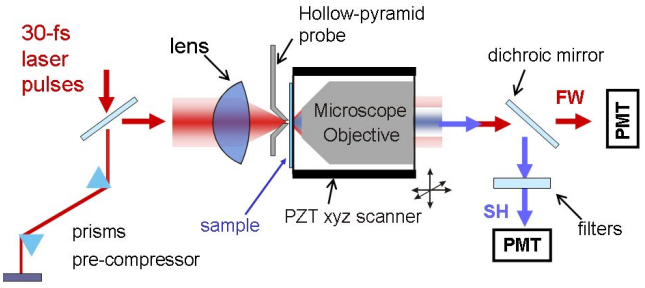

Figure 1 Schematics of our SNOM, with the ultrashort pulses coupled to the measurement head, and detection path.

2.2 Sample The sample under study consists of square arrays of gold ellipsoids produced by electron beam lithography (EBL) [25]. EBL is operated by a 30 kV Hitachi S-3500N scanning electron microscope equipped with a nanometer pattern generation system (J. C. Nabity Lithography Systems, U.S.A.). The structures are fabricated on a quartz substrate to suppress parasitic luminescence. A high resolution polymethylmethacrylate resist is spin-coated over the substrate and covered by 10 nm of aluminium. After exposure, the patterns are developed using methylisobutylketone:isopropyl alcohol (1:3) and the desired mass thickness of gold is evaporated on the sample. Lift-off is then performed using acetone. The short axis of the ellipsoids is ~70 nm long, the height is ~70 nm, the long axis can be either 100, 150 or 400 nm long, and the array period is 1 μm.

Extinction spectra of the ellipsoids (not shown here) were recorded by a modified Jobin-Yvon confocal micro-Raman spectrometer; the sample was illuminated from the bottom side and the transmitted light was collected from a 70x70 μm^2 area by a 10× microscope objective with 0.25 N.A, with the light polarized parallel to the long axes of the particles. The 100-nm long ellipsoids show a strong extinction peak at 690 nm, which shifts to 810 nm for the 150-nm long ones and to more than 1 μm for the 400-nm ones. Our excitation laser is thus tuned to be resonant with the 150-nm particles. Such peaks can be ascribed to surface plasmon resonances (SPRs) in accordance to theoretical expectations [25].

3 Results and discussion

The ability to preserve pulse duration and polarization through the hollow pyramid [21, 22] allowed us to obtain high-peak-power excitation with polarization control of both resonant and non-resonant ellipsoids. Figure 2 shows the topography of nanoellipsoids of different size [Fig. 2(a), (d) and (g)], their FW SNOM transmission maps [Figs. 2(b), (e) and (h)], and SHG SNOM emission maps [Figs. 2(c), (f) and (i)]. Incident light is polarized parallel to the long axis of the particles. In the FW maps, all the 100-nm ellipsoids appear bright, while almost all of the 150-nm ellipsoids appear dark with strong extinction hot-spots, and 400-nm ellipsoids are slightly darker than the background. In the SH images, only few of the 100-nm long particles do emit; most of the resonant 150-nm long ones emit uniformly with high contrast (up to 170%); finally, the 400-nm long particles appear darker than the substrate.

The combined analysis of the FW and SH maps of gold nanostructures allows distinguishing among diverse interaction processes occurring in the near field. The 100 nm nanoparticles do not generally display SH emission because the excitation wavelength is not resonant with their LSP, and therefore their extinction is low. They appear bright in the FW image because the amount of partially-evanescent incident FW light converted into a propagating

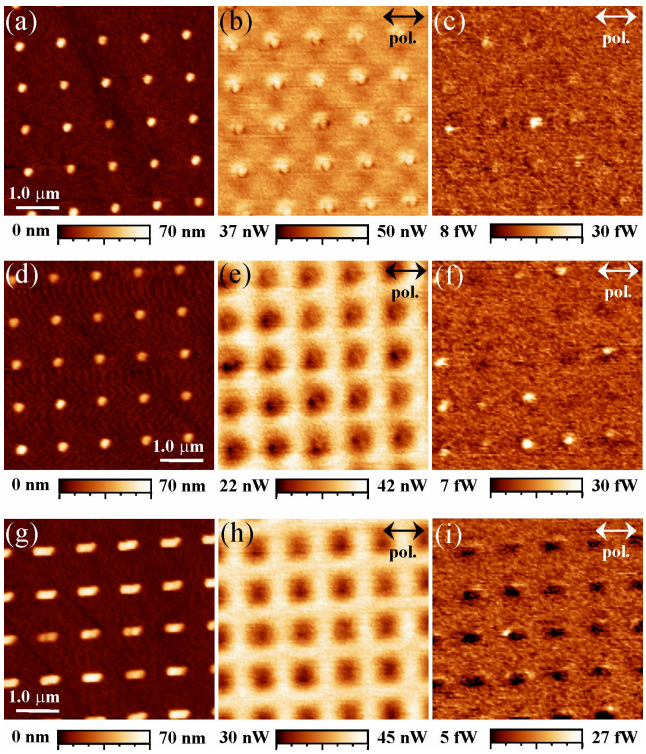

Figure 2 (a-d-g) Topography, (b-e-h) fundamental wavelength transmission, and (c-f-i) SHG-SNOM images of a 5x5 array of ellipsoids of different major axis length: 100 nm (a-b-c), 150 nm (d-e-f), 400 nm (g-h-i). Incident light is polarized parallel to such major axis.

signal by near-field interaction prevails over their weak extinction. This near-field scattering phenomenon, at variance with standard far-field scattering, is able to reduce, rather than to increase, light extinction. In addition, clear signs of interference and near-field diffraction effects can be seen, as a result of the spatial periodicity of the ellipsoids, which is not far from the excitation wavelength. The 150 nm ellipsoids have a resonant extinction behaviour, in agreement with far-field extinction spectra: they appear dark with high contrast in the FW image; moreover, they strongly emit SH as a result of the high field coupling produced by LSP excitation. The presence of a probe in the near field could in general produce a shift in LSP resonance with respect to far-field measurements. However SH maps show that, in our case, the frequency shift is small enough to still allow for efficient excitation of the LSP at 800 nm. Finally, the 400 nm ellipsoids strongly backscatter both the FW and the background SH produced by the aluminum rims of tip. This "shadowing" behaviour at both wavelengths has to do with the size of the particle, much larger than the aperture size in this case. The dark, well-resolved features appearing in the FW image at the edges of some of the 100- and 150-nm particles are artefacts produced by the aperture that "swallows" smaller particles due to its larger size.

The fact that nominally identical particles display quite similar FW emissions and very different SHG is a remarkable phenomenon. In particular, particles that emit more strongly the SH appear dark in FW images, but not all the particles appearing dark in FW maps also display SH emission, in agreement with the theoretical predictions of Ref. 15. An explanation for this behaviour can be as follows. Strong light extinction at the FW occurs when the excitation wavelength is resonant with the LSP of the nanoparticle. The resonance condition gives rise to a strong field coupling, which promotes nonlinear effects on the surface (SHG in our case). Moreover, lightning rod or other geometrical effects provide LFE at specific sites of the nanoparticle. Therefore, SHG efficiency strongly depends on both particle fine structure and excitation of LSP related to the particle size and geometry. On the other hand, the related re-emission process could arise only from symmetry-breaking due to both confined illumination and local morphology of the particles [18, 26], which in our case, display remarkable variation (checked via AFM images) due to fabrication imperfections.

The lightning-rod effect is also evident in the SH image from some of the non-resonant 400 nm particles [Fig. 2(i)], where SHG due to local strong curvatures occurs when the SNOM tip is located at the particle edges.

A further analysis of non-resonant particles shows the effect of pure morphology-dependent SHG. In Fig. 3 the comparison of FW extinction (a,b) and SHG produced by mutually orthogonal excitation polarizations (c,d) is shown. While illumination of the 400 nm-long particles with radiation polarized parallel to the major axis shows a weak interaction due to weak plasmon coupling, orthogonal polarization shows high-level and spatially confined SHG, being very sensitive to strong curvatures (optical resolution is below 100 nm with the 10%-90% criterion). This can also be tentatively ascribed to the orthogonal polarization being more confined than the parallel one at correspondence with the particle high-curvature spots, thus resulting in an increase of the LFE needed to promote nonlinear processes.

Figure 3(e) allows for the comparison – by means of chromatic superposition – between linear (black to red scale) and nonlinear (blue to white scale) optical signals and nanoparticle position (yellow dotted line). Here the purpose is to give a qualitative picture of the perfect spatial co-localization. Moreover, while particles on the left side of Fig. 3(b) and (d) show a symmetrical response in both extinction and SHG, the ones on the right have a very strong extinction spot on the left-hand side, that however is

not converted into strong SHG. The absence of SHG has to be related to imperfections, also visible in the related topographic image (not shown here). We finally remark that the simultaneous acquisition of topography, FW extinction and SHG allows for a complete picture of interactions between light and metal nanostructures at the nanometer scale.

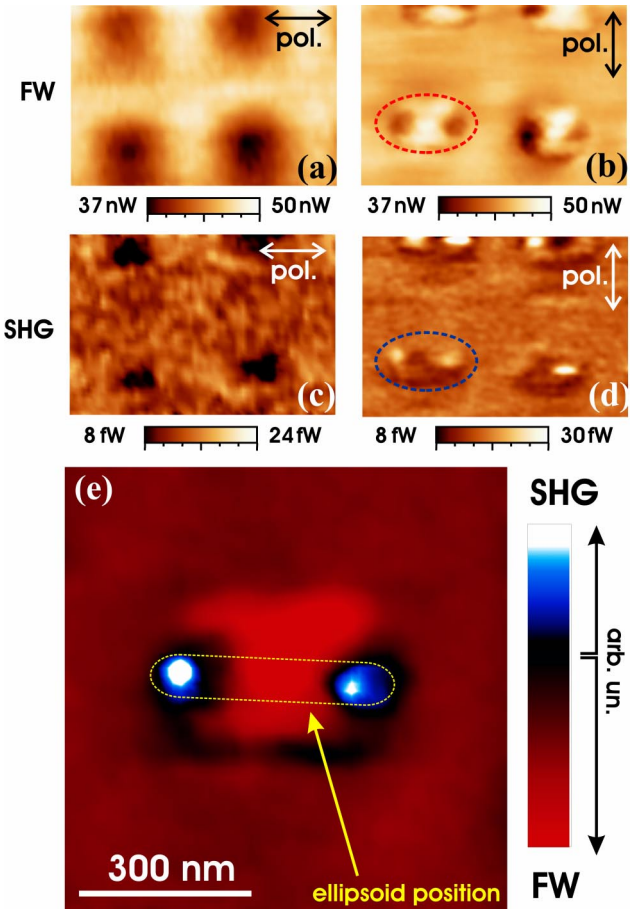

Figure 3 The effect of different polarizations on non-resonant particles (400 nm long). Excitation of long particles with polarization along their major axis shows very weak interaction in both FW (a) and SHG (c), while polarization parallel to the shorter axis induces nonlinear effects that turn out to be more sensitive to high curvature spots of the particle surface, as demonstrated by the double lobe at the particles on the left of both FW (b) and SHG (d) images. In (e) the lower-left particle in (d)-(b) (red and blue dashed lines respectively) is plotted by means of a chromatic superposition; subtraction of the two images' data is obtained after proper normalization. On (a)-(d), image size is 2.2 µm x 1.5 µm.

4 Conclusion We performed nonlinear optical experiments at the nanoscale by a hollow-pyramid aperture SNOM coupled to a femtosecond laser. High peak power light pulses in the near field allow us to locally excite SH emission from the particles, with sub-100-nm resolution and high contrast. Simultaneous topography, linear scattering and SHG mapping at the nanoscale provide unique information on LFE distribution. In particular, near-field SHG is shown to be very sensitive to LSP resonances as well as to the nanoscale morphology. The complementary acquisition of FW and SH maps allows us to correctly evaluate intensity distributions and to address scattering and absorption processes, that determine the total near-field extinction.

Acknowledgements We acknowledge financial support from the National FIRB project "Nanotechnologies and Nanodevices for the Information Society". P.-M. A. and J.G. acknowledge support from the European Community, Contract No. RII3-CT-2003-506350. We thank S. Perissinotto and V. Rouget for assistance with the software. Image processing was performed by the WSxM free software downloadable at http://www.nanotec.es.

References

[1] W. L. Barnes, A. Dereux, and T. W. Ebbesen, Nature **424**, 824 (2003).
[2] S. I. Bozhevolnyi, V. S. Volkov, E. Devaux, J.-Y. Laluet, and T. W. Ebbesen, Nature **440**, 508 (2006).
[3] P. Mühlschlegel, H.-J. Eisler, O. J. F. Martin, B. Hecht, and D. W. Pohl, Science **308**, 1607 (2005).
[4] L. Novotny and S. J. Stranick, Annu. Rev. Phys. Chem. **57**, 303 (2006).
[5] A. V. Zayats and I. I. Smolyaninov, J. Opt. A **5**, S16 (2003).
[6] I. I. Smolyaninov, A. V. Zayats, and C. C. Davis, Phys. Rev. B **56**, 9290 (1997).
[7] D. Jakubczyk, Y. Shen, M. Lal, K. S. Kim, J. Świątkewicz, and P. N. Prasad, Opt. Lett. **24**, 1151 (1999)
[8] A. V. Zayats, V. Sandoghdar, T. Kalkbrenner, and J. Mlynek, Phys. Rev. B **61**, 4545 (2000).
[9] I. I. Smolyaninov, H. Y. Liang, C. H. Lee, C. C. Davis, S. Aggarwal, and R. Ramesh, Opt. Lett. **25**, 835 (2000).
[10] Y. Shen, P. Markowicz, J. Winiarz, J. Swiatkiewicz, and P. N. Prasad, Opt. Lett. **26**, 725 (2001).
[11] A. Bouhelier, R. Bachelot, G. Lerondel, S. Kostcheev, P. Royer, and G. P. Wiederrecht, Phys. Rev. Lett. **95**, 267405 (2005).
[12] K. Imura, T. Nagahara, and H. Okamoto, Appl. Phys. Lett. **88**, 023104 (2006).
[13] J. I. Dadap, J. Shan, K. B. Eisenthal, and T. F. Heinz, Phys. Rev. Lett. **83**, 4045 (1999).
[14] S. I. Bozhevolnyi and V. Z. Lozovski, Phys Rev. B **65**, 235420 (2002).
[15] M. I. Stockman, D. J. Bergman, C. Anceau, S. Brasselet, and J. Zyss, Phys. Rev. Lett. **92**, 057402 (2004).
[16] S. I. Bozhevolnyi, J. Beermann, and V. Coello, Phys. Rev. Lett. **90**, 197403 (2003).
[17] J. Beermann and S. I. Bozhevolnyi, Phys. Rev. B **69**, 155429 (2004).
[18] B. K. Canfield, S. Kujala, K. Laiho, K. Jefimovs, J. Turunen, and M. Kauranen, Opt. Express **14** , 950 (2006.)
[19] D. W. Pohl, W. Denk, and M. Lanz, Appl. Phys. Lett. **44**, 651 (1984)
[20] A. V. Zayats and V. Sandoghdar, Opt. Commun. **178**, 245 (2000).

[21] M. Labardi, M. Zavelani-Rossi, D. Polli, G. Cerullo, M. Allegrini, S. De Silvestri, and O. Svelto, Appl. Phys. Lett. **86**, 031105 (2005).
[22] P. Biagioni, D. Polli, M. Labardi, A. Pucci, G. Ruggeri, G. Cerullo, M. Finazzi, and L. Duò, Appl. Phys. Lett. **87**, 223112 (2005).
[23] Witec GmbH, Ulm, Germany
[24] M. Celebrano, M. Zavelani-Rossi, D. Polli, G. Cerullo, P. Biagioni, M. Finazzi, L. Duò, M. Labardi, M. Allegrini, J. Grand, and P.-M. Adam, J. Microsc., in press.
[25] J. Grand, M. Lamy de la Chapelle, J.-L. Bijeon, P.-M. Adam, A. Vial, and P. Royer, Phys. Rev. B **72**, 033407 (2005).
[26] M. Finazzi, P. Biagioni, M. Celebrano, and L. Duò, Phys. Rev. B **76**, 125414 (2007).